

Supporting Information for
Visualizing Subcellular Enrichment of Glycogen in Live Cancer Cells by Stimulated Raman Scattering

Dongkwan Lee¹, Jiajun Du¹, Rona Yu², Yapeng Su^{1,3}, James R. Heath³, Lu Wei^{1*}.

¹Division of Chemistry and Chemical Engineering, California Institute of Technology, Pasadena, CA, USA.

²Division of Engineering and Applied Science, California Institute of Technology, Pasadena, CA, USA.

³Institute of Systems Biology, Seattle, WA, USA

*email: lwei@caltech.edu.

Table of Contents

Supplementary Figures S1-S15

pages S2-S16

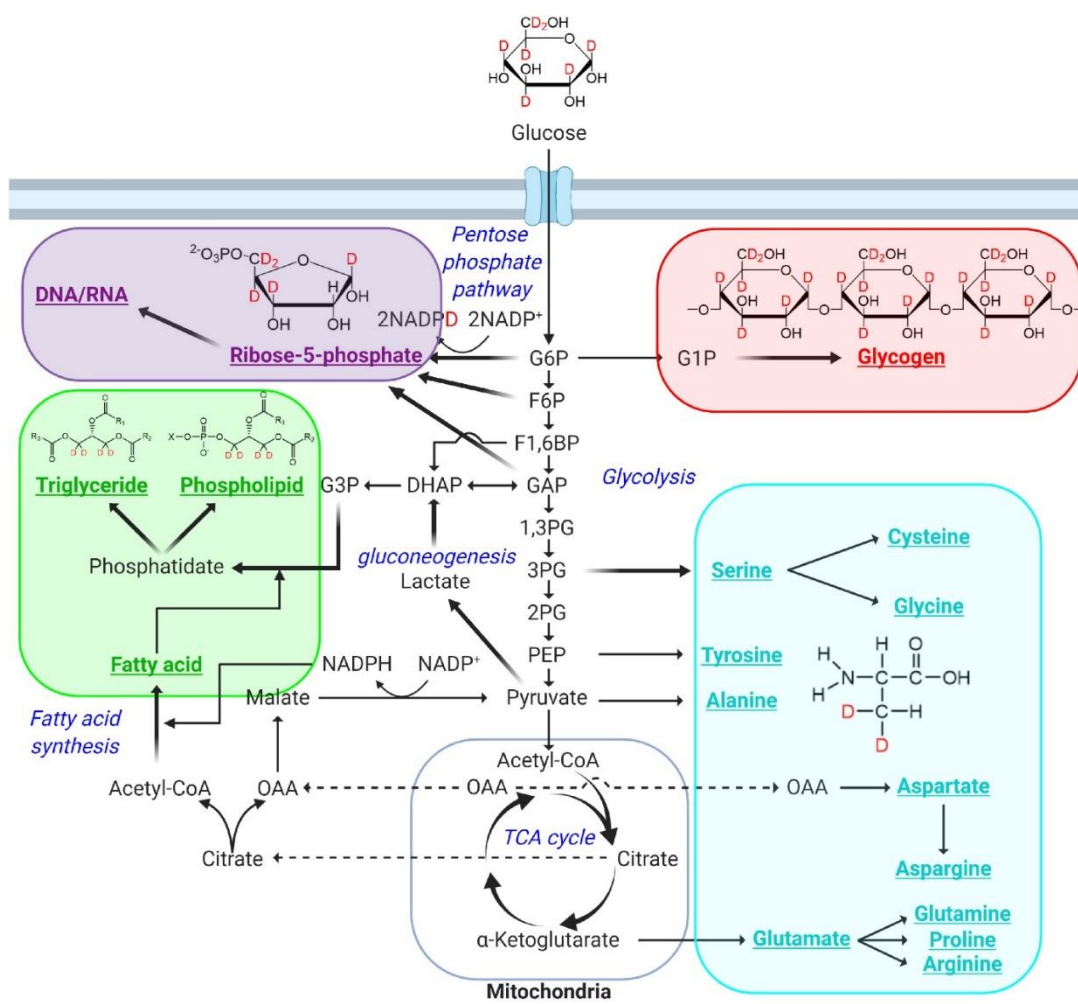


Fig. S1. Sparse C-D labeling of macromolecules (glycogen, DNA/RNA, lipid, and protein) through metabolic pathways branched from glycolysis of d_7 -glucose. Glycogen, DNA/RNA, lipid and protein are highlighted in red, purple, green, and cyan, respectively. OAA: oxaloacetate.

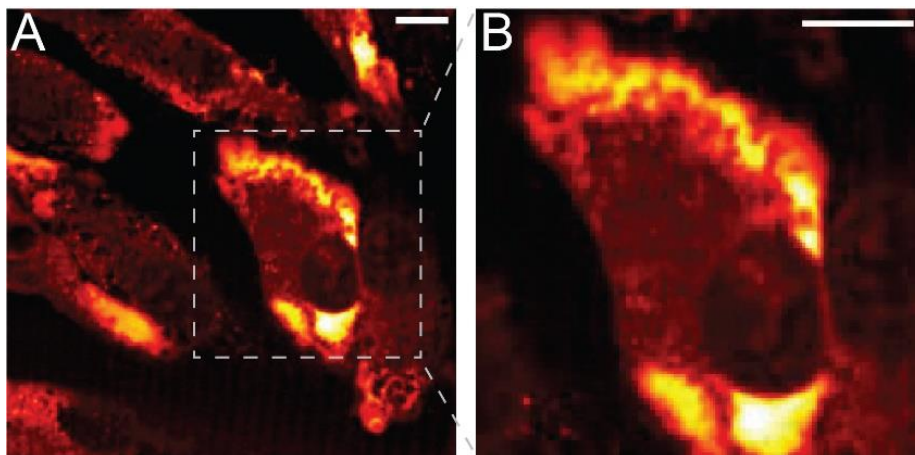


Fig. S2. A higher-magnification image of intracellular glycogen pools. (A) A SRS image at 2151 cm^{-1} for HeLa cells after incubating in d_7 -glucose media for 3 days. (B) A zoomed-in image of the boxed-region in (A). Scale bars, $10\text{ }\mu\text{m}$.

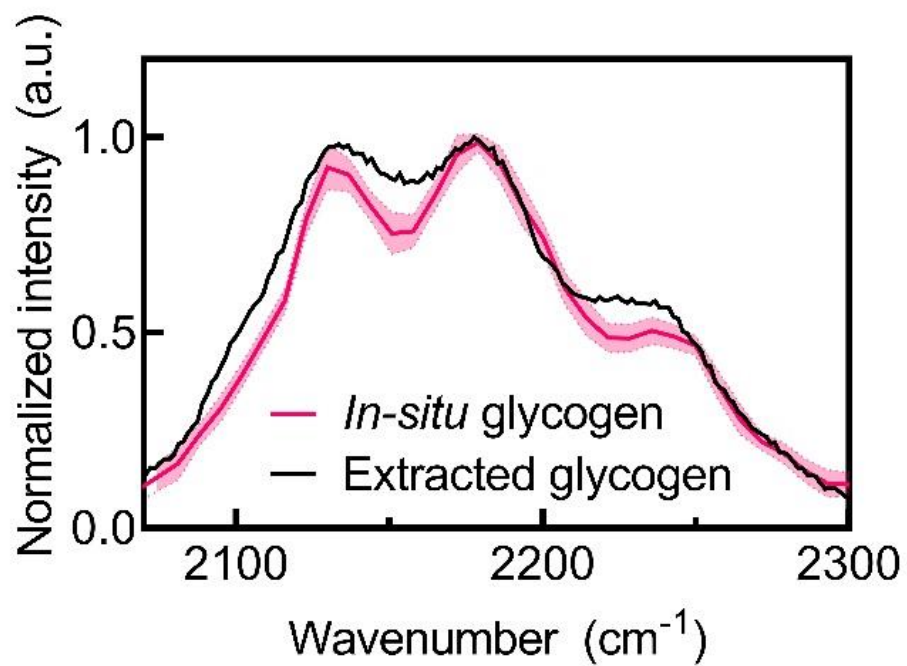


Fig. S3. Comparison between *in-situ* SRS spectra from bright spots and spontaneous Raman spectra of extracted deuterated glycogen.

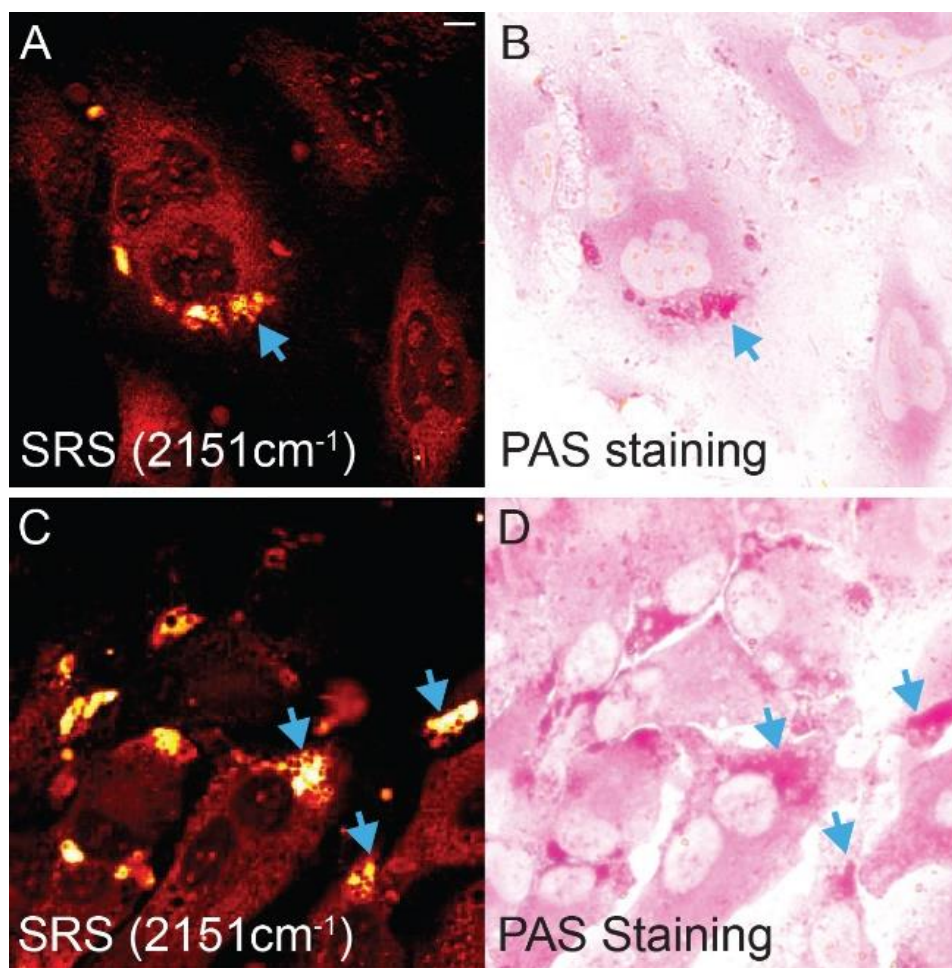


Fig. S4. Two sets of correlative imaging of glycogen. (A) & (C) SRS images of glycogen in HeLa cells incubated with d₇-glucose for three days. (B) & (D) Brightfield images of the same set of cells in (A) and (B), respectively, after PAS staining. Blue arrows indicate the glycogen pools.

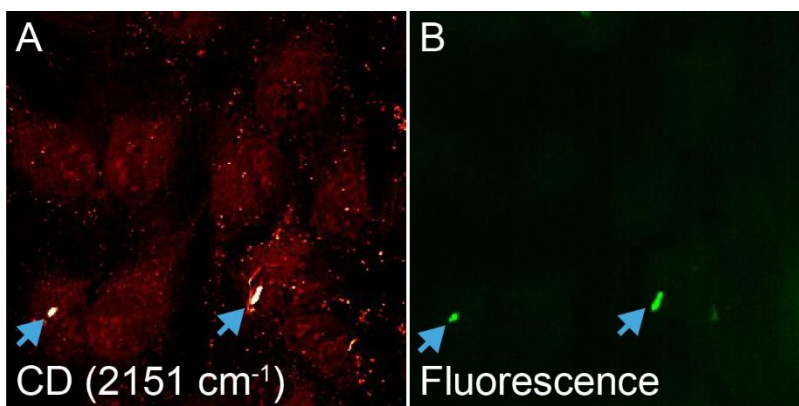


Fig. S5. Correlative imaging of glycogen. (A) SRS image of glycogen in HeLa cells incubated with d₇-glucose for three days and immuno-labeled with anti-glycogen primary antibody and Alexa Fluor 594-conjugated secondary antibodies. (B) Fluorescence image of the same set of cells in (A). Blue arrows indicate the glycogen pools.

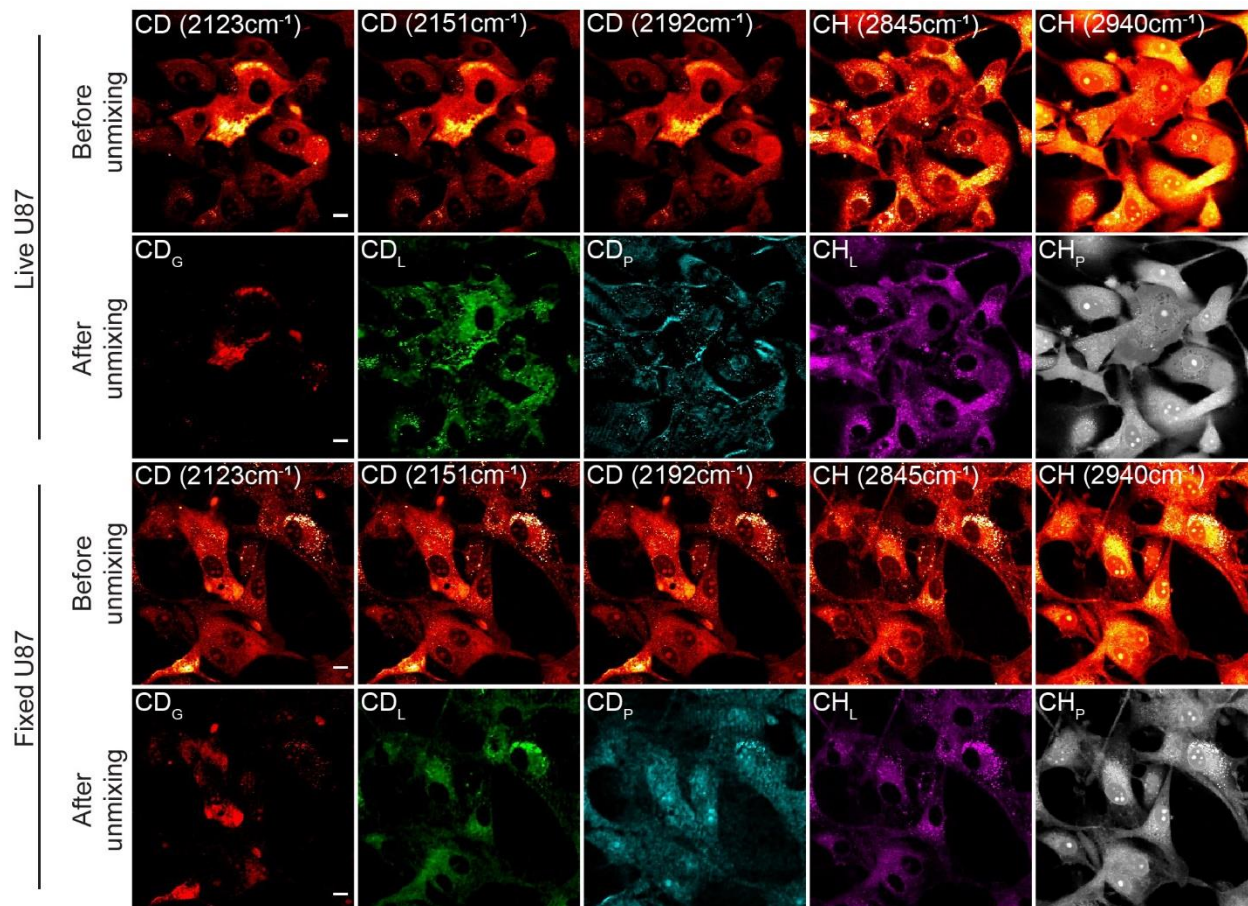


Fig. S6. Spectral unmixing of deuterated glycogen, lipid, and protein macromolecules in live and fixed U87 cells. Concentration maps for d_7 -glucose-derived glycogen (CD_G , red), lipids (CD_L , green), and proteins (CD_H , blue) (after unmixing) are spectrally separated from SRS images acquired at channels of 2123, 2151, 2192 cm^{-1} (before unmixing). Pre-existing lipid (CH_L , purple) and protein (CH_P , gray) signals (after unmixing) are unmixed from images collected at 2845, 2940 cm^{-1} (before unmixing). Scale bars, 10 μm .

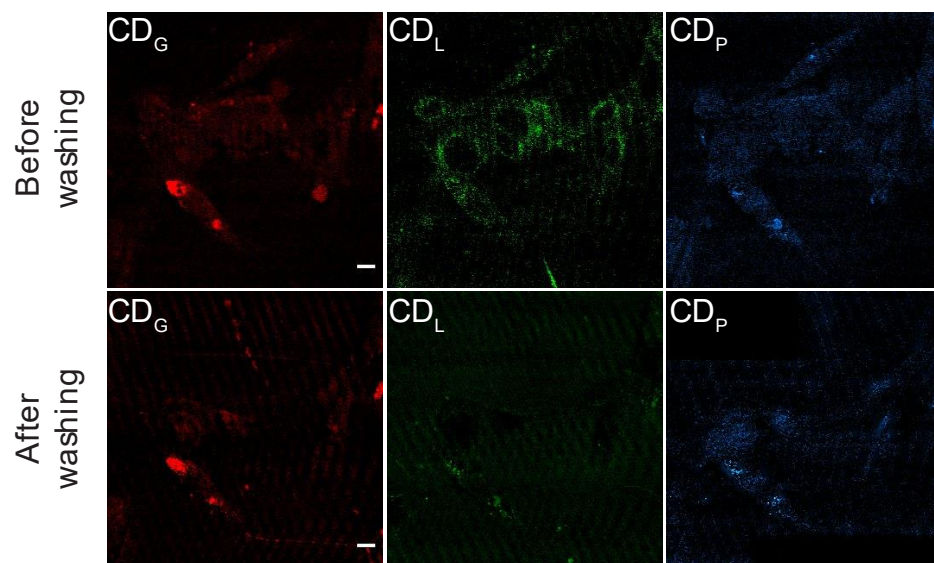


Fig. S7. Unmixed SRS images before and after lipid washing using triton. SRS images collected at 2123, 2151, 2192 cm^{-1} and unmixed into glycogen (CD_G , red), lipid (CD_L , green), and protein (CD_H , blue) signals.

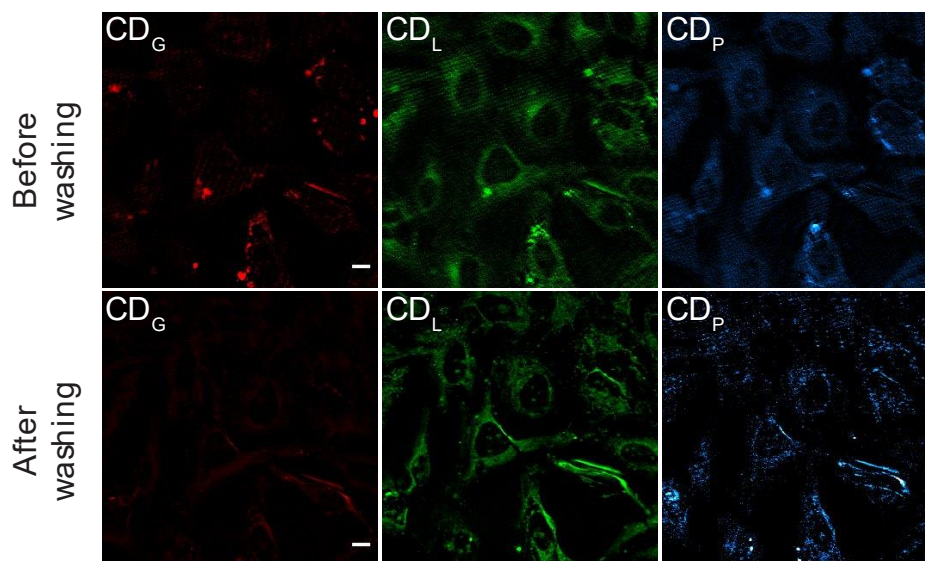


Fig. S8. Unmixed SRS images before and after glycogen washing using perchloric acid. SRS images collected at 2123, 2151, 2192 cm^{-1} and unmixed into glycogen (CD_G , red), lipid (CD_L , green), and protein (CD_H , blue) signals.

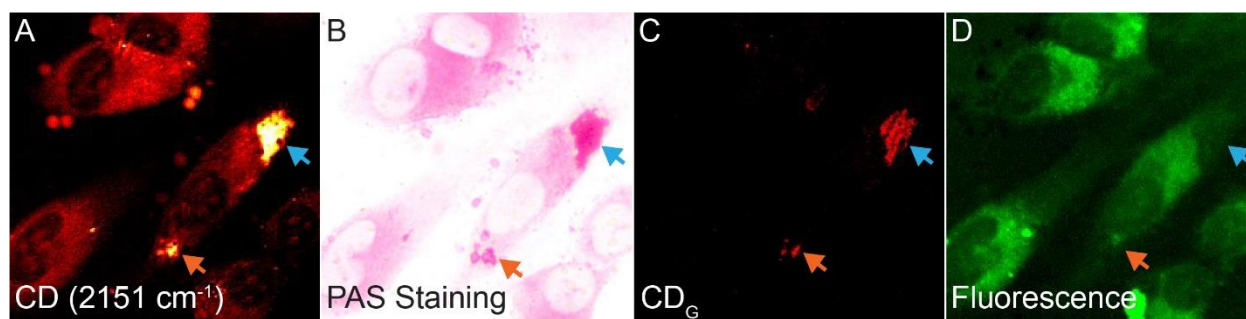


Fig. S9. 3-channel correlative imaging of glycogen in fixed HeLa cells co-incubated with d7-glucose (25 mM, 65 hours) and 2-NBDG (100 μ M for the last 18 hours). (A) The SRS image. (B) The brightfield image on the same set of cells after applying PAS staining. (C) Glycogen SRS (CD_G) channel after spectral unmixing. (D) The fluorescence image of 2-NBDG. The Orange arrows indicate regions of correlation between all three SRS, PAS, and fluorescence images. The Blue arrows indicate regions of high correlation between SRS image and PAS staining but not from fluorescence image.

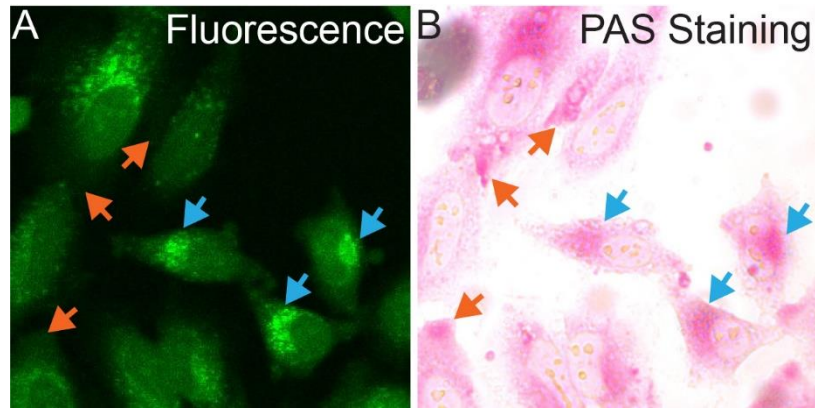


Fig. S10. 2-channel correlation imaging for PAS staining and 2-NBDG labeling on HeLa cells starved for 12 hours first and then incubating with 500 μ M of 2-NBDG for 3 hours. (A) Fluorescence imaging of 2-NBDG. (B) Brightfield imaging on the same set of cells in (A) after applying PAS staining. Blue arrows indicate regions with correlation. Orange arrows indicate regions that lack correlation. The non-correlation between fluorescence and the PAS image was not due to the z shift, as all the z was checked.

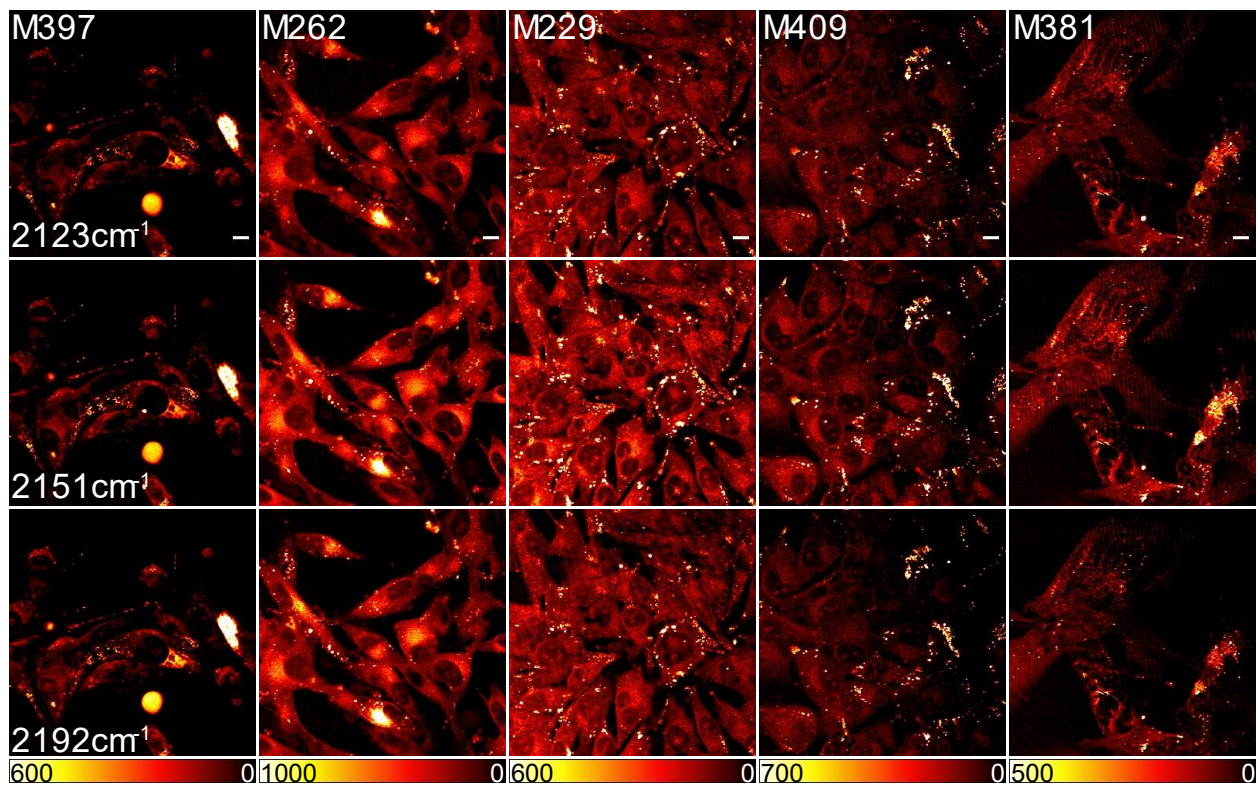


Fig. S11. Representative SRS images of melanoma cell-lines before spectral unmixing. Each column indicates the representative image set on the same set of cells for one cell-line. Scale bar, 10 μm

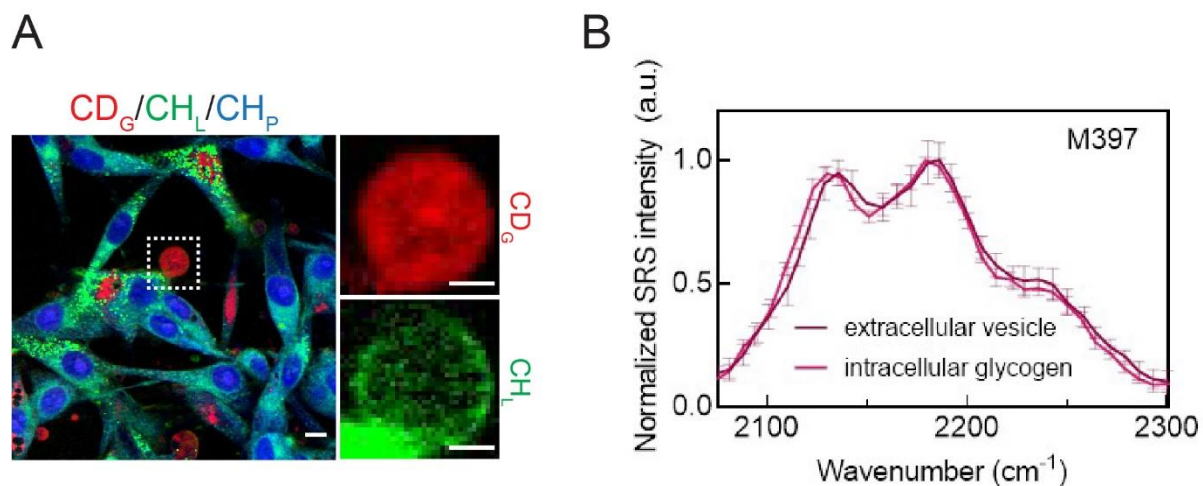


Fig. S12. PFA fixation induces glycogen-enriched extracellular vesicles. (A) Overlay of CH_L, CH_P and CD_G images for PFA-fixed M397 cells. Scale bar, 10 μm. Zoomed-in images of the dashed-boxed region indicate a representative extracellular vesicle enriched with glycogen (CD_G, red) and wrapped by the lipid membranes (CH_L, green). Scale bars, 5 μm. (B) Normalized SRS spectra from intracellular glycogen (shaded pink) and extracellular vesicles (shaded purple) in PFA-fixed M397 cells.

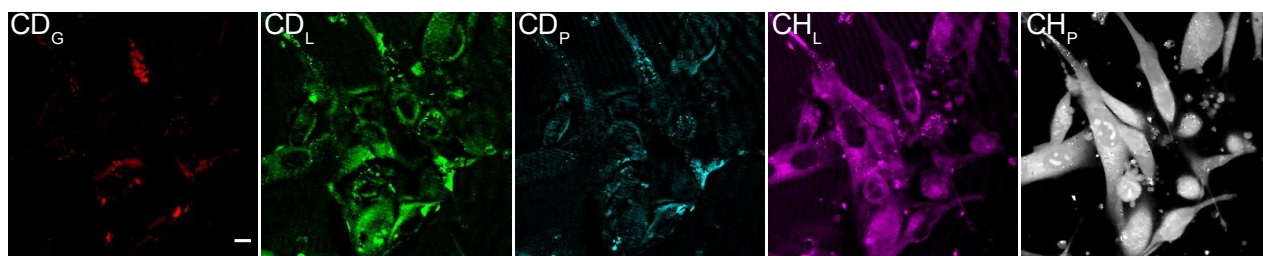


Fig. S13. No glycogen-enriched extracellular vesicles were observed in live M397 cells. Concentration maps for d₇-glucose-derived glycogen (CD_G, red), lipid (CD_L, green), and protein (CD_H, blue) after unmixing. Pre-existing lipid (CH_L, purple) and protein (CH_P, gray) signals (after unmixing) are unmixed from images collected at 2845, 2940 cm⁻¹. Scale bars, 10 μm.

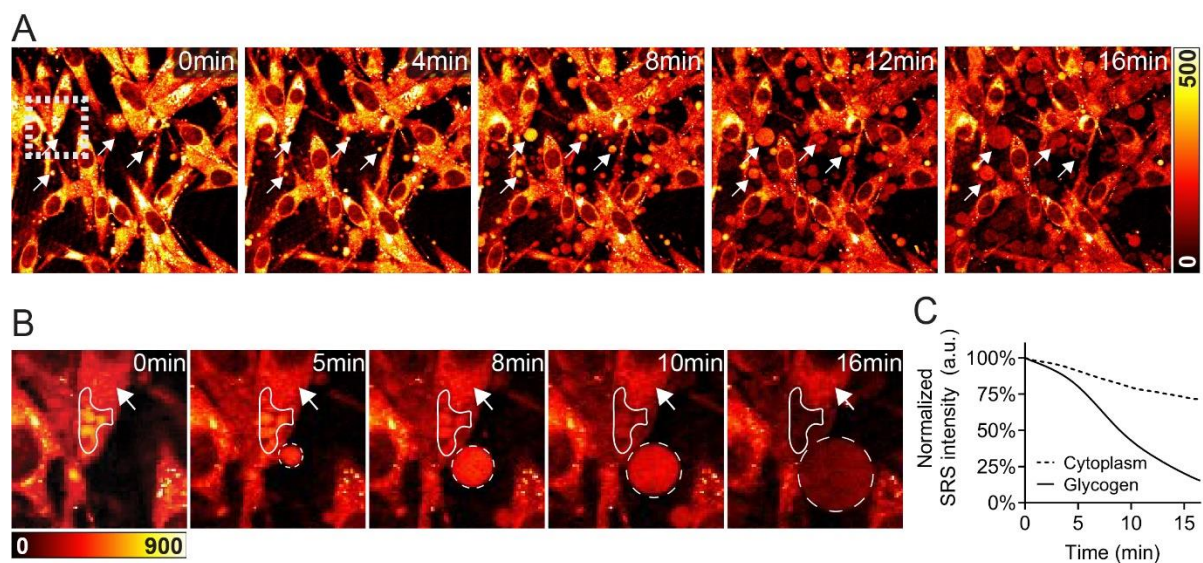


Fig. S14. Observation of glycogen-enriched extracellular vesicles formation and intracellular glycogen loss caused by PFA fixation. (A) Time-lapse SRS images from 0 to 16 minutes immediately after adding PFA to M397 cells. Formation of glycogen-enriched vesicles is indicated by arrows. (B) Zoomed-in images of the boxed-region in (A). Intracellular glycogen is outlined by solid lines. Extracellular vesicles are indicated by dashed circles. Arrows indicate cytoplasm with no glycogen. (C) Quantification of SRS intensities from intracellular glycogen (solid lined) and extracellular vesicles (dashed circled) highlighted in (B). With the secretion of vesicles, the signal levels of intracellularly accumulated glycogen decreased sharply to about only 20% of the original signals, whereas the cytoplasmic signals where glycogen was not present only decreased slightly to about 75%.

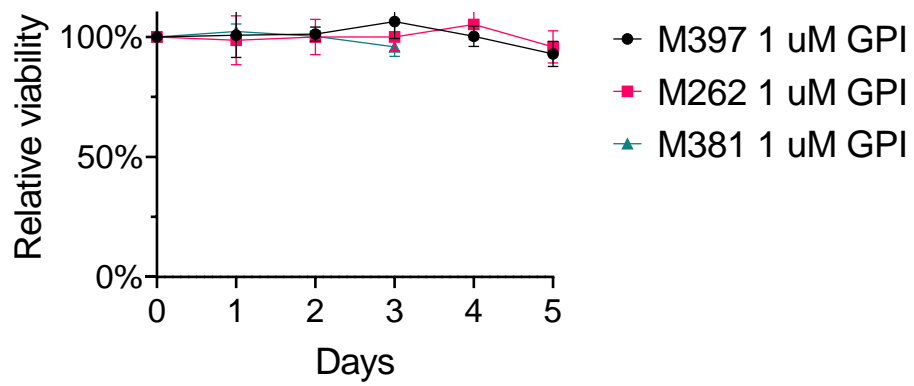


Fig. S15. Non-toxicity from GPI are found in normal glucose containing medium.